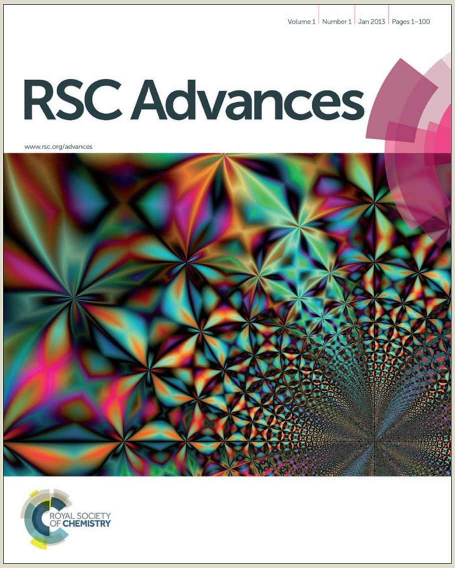
Volume 1 | Number 1 | Jan 2013 | Pages 1–100
RSC Advances
www.rsc.org/advances
ROYAL SOCIETY OF CHEMISTRY

Cite this: DOI: 10.1039/c0xx00000x

www.rsc.org/xxxxxx

ARTICLE TYPE

Green synthesis of polypyrrole-supported metal catalysts: application to nitrate removal in water

M. Jesús García-Fernández,[a] Robison Buitrago-Sierra,[a] M. Mercedes Pastor-Blas,[a] O.S.G.P. Soares,[b] M.F.R. Pereira,[b] and Antonio Sepúlveda-Escribano*[a]

Received (in XXX, XXX) Xth XXXXXXXXX 20XX, Accepted Xth XXXXXXXXX 20XX
DOI: 10.1039/b000000x

Pt and Pt/Sn catalysts supported on polypyrrole (PPy) have been prepared using Ar plasma to reduce the metal precursors dispersed on the polymer. The PPy support was synthesized by chemical polymerization of pyrrole with $FeCl_3 \cdot 6H_2O$, this leading to the conducting form of the polymer (conductimetric measurements). The Ar plasma treatment produced a partial reduction of platinum ions, anchored as platinum chloro-complexes to the PPy chain, into metallic platinum. A homogeneous distribution of Pt and Sn nanoparticles was observed by TEM. Activity of the PPy-supported catalysts was evaluated in the reduction of aqueous nitrate with H_2 at room temperature. Nitrate concentration in water below the maximum acceptable level of 50 $mg \cdot L^{-1}$ was achieved with all catalysts. However, considering not only efficiency in nitrate reduction, but also minimized concentrations of undesired nitrite and ammonium, the monometallic Pt catalyst seems to be the most promising one.

Introduction

Nitrate (NO_3^-) is a naturally occurring form of nitrogen found in soil which is formed as a part of the nitrogen cycle. Plants use nitrates from the soil to satisfy nutrient requirements and may accumulate nitrate in their leaves and stems. Due to its high mobility, nitrate also can leach into groundwater. In moderate amounts, nitrate is a harmless constituent of food and water. However, if people or animals drink water with a high content in nitrate, it may cause methemoglobinemia, or blue baby syndrome, an illness found especially in infants,[1] and even cancer. Nitrate values are commonly reported as either nitrate (NO_3^-) or as nitrate-nitrogen (NO_3^--N). The maximum contaminant level (MCL) in drinking water as nitrate (NO_3^-) is 50 $mg \cdot L^{-1}$, whereas as nitrate-nitrogen (NO_3^--N), which relates to the actual nitrogen in nitrate, is 11.3 $mg \cdot L^{-1}$.[2,3]

Although the term "nitrate toxicity" is commonly used, the toxic principle is actually nitrite. Nitrate is converted to nitrite in the stomach. Nitrite is absorbed from the stomach and converts blood hemoglobin to methemoglobin, which cannot transport oxygen to body tissues, thus causing death.

While it is technically possible to treat contaminated groundwater, it can be difficult, expensive and not totally effective. Charcoal filters and water softeners do not adequately remove nitrates from water. Boiling nitrate-contaminated water does not make it safe to drink and, actually, this treatment increases the concentration of nitrates. Other water treatments include distillation, reverse osmosis and ion exchange. These technologies transfer nitrates from water to a concentrate phase that requires further treatment or disposal. In this way, catalytic reduction of nitrates with H_2 using supported metal catalysts has been proposed as an alternative.

Nitrate reduction progresses through nitrite (NO_2^-) and daughter intermediates (e.g. nitric oxide (NO) and nitrous oxide (N_2O)), which are then reduced to dinitrogen (N_2) and ammonium (NH_4^+). Considering the toxicity of ammonium, a catalyst which is highly selective to nitrogen must be developed. It has been reported[4-6] that initial reduction of NO_3^- to NO_2^- requires a bimetallic catalyst (a noble metal as Pd, combined with a secondary promoter metal as Cu, In, Sn, Co). The intermediate NO_2^- can then be further reduced on monometallic sites. It is also known that the catalytic behavior is affected by the support[7]. Carbonaceous supports (activated carbon, carbon nanotubes),[8] metal oxides such as TiO_2 ,[9] SiO_2,[10] Nb_2O_5,[11] SnO_2,[12] ZrO_2,[13] Al_2O_3,[14] TiO_2,[15] CeO_2, [16] zeolites[17] and hydrotalcites[18] have been proposed as supports for the catalyzed reduction of nitrate[19-22]. In this work, the properties of a conducting polymer (polypyrrole) as the catalytic support have been assessed. Polypyrrole can easily change between its reduced (non-conducting) and oxidized (conducting) forms. This feature makes it interesting to prepare supported catalysts by impregnation of a metal salt, as electrons from the polymeric chain may be transferred to the metallic ion promoting its reduction[23]. Considering their limited thermal stability, applications of polymer-supported catalysts are restricted to low temperature reactions. In this work, activity and selectivity of monometallic (Pt) and bimetallic (Pt:Sn) catalysts supported on polypyrrole have been determined in the reduction of nitrate in water with H_2 as the reducing agent. The use of plasma is a powerful method to synthesize nanoparticles. Hydrogen atmospheric dielectric-barrier plasma has been used to reduce supported Pt and Co Catalysts. [24] Since reduction is an electron transfer process, and plasma reduction treatment is based in a direct transfer of high energy electrons from the plasma to the metal ions, it should be possible to use other gases such as helium and argon as reducing agents instead of hydrogen. In this study, the activation of the catalysts to obtain metal nanoparticles has been carried out by the environmentally friendly cold argon plasma treatment.[23]

Experimental

Materials preparation

Polypyrrole was prepared by chemical polymerization of pyrrole with ferric chloride ($FeCl_3·6H_2O$) as the oxidant. 9 g of $FeCl_3·6 H_2O$ (33 mmol) were dissolved in 200 mL of ultrapure water resulting in an orange solution. Then, 1 mL of pyrrole (C_4H_5N) (98%, Sigma-Aldrich) was added drop wise (oxidant to pyrrole molar ratio: 2.33) and the solution was stirred for 6 h at room temperature. As soon as pyrrole was mixed with the $FeCl_3$ solution it turned to its characteristic black color, this indicating the formation of polypyrrole (PPy). The precipitated polypyrrole powder was filtered, washed with distilled water and dried at 80 °C for 12 h.

The monometallic PPy-supported platinum catalyst was prepared by wet impregnation in excess of solvent, using $H_2PtCl_6·6H_2O$ as the metal precursor. Thus, the proper amount of this salt to obtain 2 wt.% Pt loading was dissolved in ultrapure water, and then it was contacted with polypyrrole (25 mL solution/g_{PPy}). Bimetallic catalysts were prepared by co-impregnation with $H_2PtCl_6·6H_2O$ (2 wt.% Pt) and $SnCl_2·2H_2O$ aqueous solutions in Pt:Sn atomic ratios 3:1 and 1:1. In all cases, the suspensions were stirred for 12 h at room temperature and then the solvent was evaporated under reduced pressure in a rotary evaporator. The polypyrrole-supported catalyst precursor was dried in an oven at 80 °C for 12 h and then, the obtained material was splitted in two portions, one of them to be characterized and the other one to be treated by Ar plasma.

Plasma treatment proceeded as follows: the polypyrrole-supported catalysts were loaded on an aluminum boat, which was placed in the glow discharge stainless steel cylindrical chamber of a Tucano plasma system (Gambetti Kenologia, Italy), provided with an anodized aluminum door. The HF electrode is made of aluminum and has a “Dark Shield”, a RF 13.56 MHz power supply and mass flow controllers (MFC) for gas inlet control. The reaction chamber was evacuated to mild vacuum (0.15 Torr) using a Pfeiffer rotary vane pump model PK D41 029C-Duo 2.5 with F4 Fomblin lubricant YL VAC 25/6). Ar was introduced into the plasma chamber over the specimen. Care was taken to pump down and purge the plasma reactor for at least 10 min prior to activating the RF field. The discharge power was set to 200 watts and 36 cycles of 5 min each were applied to each sample (180 min treatment in total) with manual mixing of the sample between treatments to assure an even exposure to the plasma. The temperature of the sample after the plasma treatment was measured by a non-contact infrared thermometer (PCE Instruments, model PCE-888). It could be determined that the surface temperature was below 50 °C in all cases.

Materials characterization

The polypyrrole support (PPy) and the catalysts (PPy/Pt) and (PPy/Pt:Sn) were characterized by different techniques, both before and after the plasma treatment.

Textural characterization of polypyrrole was obtained by N_2 adsorption at -196 °C with a Coulter Omnisorp 100CX equipment. Before measurements, samples were outgassed at 150 °C for 4 h.

X-Ray diffraction (XRD) pattern of polypyrrole was obtained with a D8-Advance (Bruker) X-ray diffractometer equipped with Göebel mirror and a Cu anode which provides K_α radiation (λ = 1.5406 Å). The samples were scanned from 2θ = 6 ° to 90 ° at the step scan mode (step size 1 °, step time 3 s).

Electrical conductivity was calculated from the resistance data. Electrical resistance of polypyrrole was determined in a four-points probe home-made equipment which consisted in a cylindrical Teflon sample holder, connected to a 2000 Multimeter (Madrid, Spain) through copper electrodes. This device permitted to characterize the powered as-synthesized polypyrrole.

ATR-IR spectra were recorded on a Tensor 27 spectrophotometer (Bruker optics, Billerica, MA USA) in the 600-4000 cm^{-1} range using a zinc selenide crystal. 200 scans and a resolution of 4 cm^{-1} were used.

X-ray photoelectron spectroscopy (XPS) analysis was used to obtain information on the chemical properties of surface atoms, in particular the oxidation state of platinum loaded to the polypyrrole support and the chemical state of nitrogen in PPy. A K-Alpha spectrometer (Thermo-Scientific) spectrometer with an Al K_α achromatic X-ray source (1486.6 eV) operating at 50 keV pass energy and 300 Watt was used. The pressure inside the analysis chamber was held below $5·10^{-9}$ mbar during the course of the analysis. The measurements were taken using a take-off angle of 45º. Survey scans were taken in the range 0-1350 eV, and high resolution scans were obtained on all significant peaks in the survey spectra. The intensities were estimated by calculating the integral of each peak, after subtraction of the S-shaped background, and by fitting the experimental curve to a combination of Lorentzian (30%) and Gaussian (70%) lines. Binding energies (B.E.) were referenced to the C 1s photopeak position for C-C and C-H species at 284.5 eV, which provided binding energy values with an accuracy of ± 0.2 eV.

Transmission electron microscopy (TEM) images were taken with a JEM-2010 (JEOL Ltd., Tokyo, Japan) equipment operating at 120 kV. Sample material was mounted on a holey carbon film supported on a Cu grid by drying a droplet of an aqueous suspension of ground sample on the grid. EDX coupled to the TEM microscope provided elemental analysis of the samples.

Catalysts evaluation

The catalytic activity of the polypyrrole-supported catalysts obtained after treatment in Ar plasma at 200 watts was evaluated in the aqueous reduction of nitrate with H_2 at room temperature. A semi-batch reactor equipped with a magnetic stirrer (700 rpm) was fed with 592.5 mL of ultrapure water and 300 mg of catalyst. H_2 was used as a reducing agent and a CO_2 flow was employed as a buffer to keep a constant value of pH ~ 5 during the reaction. H_2 and CO_2 were passed for 15 min through the reactor with flow rates of 75 $cm^3 \cdot min^{-1}$ each one to assure removal of oxygen. Afterwards, 7.5 mL of a solution of $NaNO_3$ was added to the reactor (initial concentration of NO_3^- in the reactor was 100 $mg \cdot L^{-1}$). Aliquots (1 mL) were withdrawn at different times from the reactor and immediately filtered for determination of nitrate, nitrite and ammonium concentrations by ion chromatography using a Metrohm 850 ProfIC AnCat-MCS equipment. Nitrate and nitrite anions were determined in a Metrosep ASSUPP-7 column (250 mm x 4 mm) and ammonium cations were determined in a Metrosep C3 column (250 mm x 4 mm). Nitrate conversion was calculated as:

$$X_{NO_3^-} = \frac{[NO_3^-]_o - [NO_3^-]_t}{[NO_3^-]_o} \cdot 100$$

where $[NO_3^-]_0$ is the initial nitrate concentration ($mg \cdot L^{-1}$) and $[NO_3^-]_t$ is the nitrate concentration ($mg \cdot L^{-1}$) at time *t* (min).

Selectivities to NO_2^- and NH_4^+ were calculated as:

$$S_{NO_2^-} = \frac{(n_{NO_2^-})_t}{(n_{NO_3^-})_o - (n_{NO_3^-})_t} \cdot 100$$

$$S_{NH_4^-} = \frac{(n_{NH_4^+})_t}{(n_{NO_3^-})_o - (n_{NO_3^-})_t} \cdot 100$$

where $(n_{NO_3^-})_0$ is the initial amount initial amount of nitrate (mol) and $(n_{NO_3^-})_t, (n_{NO_2^-})_t, (n_{NH_4^+})_t$ are the amounts of the respective species (mol) at time *t*.

The absence of metal leaching was checked by Inducted Coupled Plasma Mass Spectrometry (ICP-MS) in aliquots withdrawn from the reactor once the nitrate reduction reaction was completed. A 7700x equipment (Agilent) was used: RF power 1150 W, He flow of 0.99 $L \cdot min^{-1}$ and liquid flow of 0.3 $mL \cdot min^{-1}$).

Results and discussion

Characterization of polypyrrole

Synthesized polypyrrole (PPy) has a BET surface area of 4 $m^2 \cdot g^{-1}$, obtained from N_2 adsorption at -196 °C. The X-ray diffraction patterns (Fig. 1) show that synthesized polypyrrole and also the prepared catalysts are mainly amorphous. All studied samples have a broad peak centered at $2\theta = 24.95°$, and a shoulder at $2\theta = 16.45°$ due to the scattering from PPy chains at the interplanar spacing between pyrrole groups.[25] Additionally, polypyrrole impregnated with Pt and Sn precursors shows a sharp peak at $\theta = 33.00°$, which is more evident when the Pt:Sn ratio is 1:1, and corresponds to the scattering of platinum ions anchored to N in polypyrrole.[23] Therefore, this platinum chloro-complex induces a more ordered arrangement of the polypyrrole chains. The d-spacing calculated from the Bragg's equation is 0.36 nm, and the average crystallite size has been estimated from the full width at half maximum (FWHM) using the Scherrer's equation, and it results in 1.7 nm.

Conductivity of polypyrrole depends of the counter-ion, the doping level and the polymer synthesis conditions; so, different conductivity values are reported in the literature: $4.9 \cdot 10^{-4}$ $S \cdot cm^{-1}$ [26], $3.6 \cdot 10^{-2}$ $S \cdot cm^{-1}$ [27] and 8 $S \cdot cm^{-1}$.[28] In this study, synthesized polypyrrole shows a conductivity of $4.5 \cdot 10^{-2}$ $S \cdot cm^{-1}$. All polypyrrole-supported monometallic and bimetallic catalysts show conductivities between 10^{-3} and 10^{-4} $S \cdot cm^{-1}$.

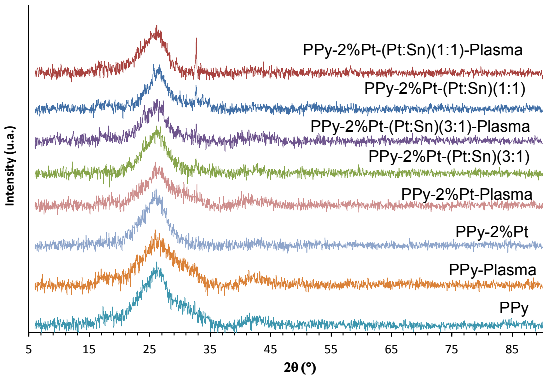

Fig. 1. XRD patterns of the different samples.

The FTIR spectrum of PPy (Fig. 2a) shows the typical bands of this material (Table 1). Insolubility of the chemically synthesized polypyrrole indicates that reticulation of polymeric chains has been produced during chemical oxidative polymerization, due to a high concentration of cationic polymeric radicals. Some degree of surface oxidation is detected (band at 1694 cm^{-1} of C=O stretching) which may be due to polypyrrole backbone oxidation through free radical oxygen insertion, and may also be produced by exposure of the polymer to air. IR spectrum of polypyrrole after impregnation with $H_2PtCl_6 \cdot 6H_2O$ (Fig. 2b) shows differences in bands of C=N-C at 1530, 1174 and 898 cm^{-1} and N-H stretching at 779 cm^{-1}. This suggests that platinum may interact with the polypyrrole chain through the nitrogen atom, which is consistent with previous results.[23]

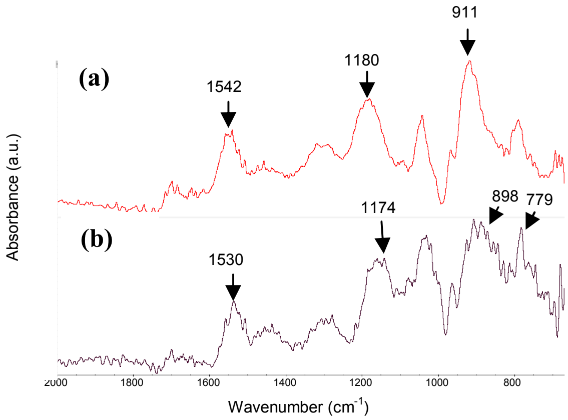

Fig. 2. FTIR-ATR spectra of (a) as-synthetized polypyrrole (PPy) and (b) polypyrrole impregnated with H_2PtCl_6 (PPy-2%Pt).

Table 1. IR bands assignment.

PPy (cm^{-1})	PPy-2%Pt (cm^{-1})	Assignment[a]
1694	1699	C=O st
1542	1530	C=N st
1450	1421	C=C st
1285	1269	C-C st
1180	1174	C-N st
1044	1024	=C-H δ_{oop}
911	898	C=N-C δ
787	779	N-H δ

[a] Stretching (st), in-plane bending (δ) and out-of-plane bending (δ_{oop}).

XPS analysis of chemically synthesized polypyrrole (Supporting information Table 1) shows C and N from the polymeric chain, as well as Cl from the $FeCl_3$ oxidant used for the chemical polymerization of polypyrrole. The analysis of the C 1s (Supporting information Fig. 1a) and O 1s (Supporting information Fig. 1b) level shows the presence of C=O and C-O moieties (Supporting information Tables 2 and 3), which supports PPy degradation and/or surface oxidation.[23] On the other hand, the N 1s spectra (Fig. 3, Supporting information Table 4) shows the presence of =N- (399.7 eV) and -NH- (400.3 eV) species in polypyrrole.

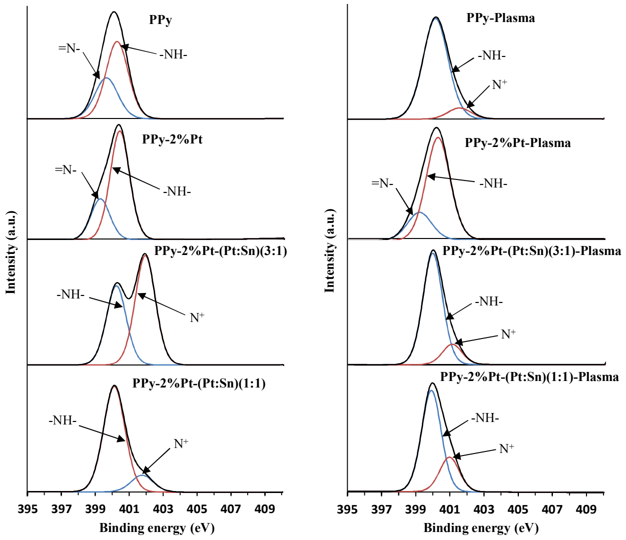

Fig. 3. Curve fit of N 1s level in XPS spectra of different samples.

Previous studies[23] have shown that impregnation of polypyrrole with H_2PtCl_6 produces the anchoring of the platinum chloro-complex on the polypyrrole by interaction with the N moieties in the polymer structure, together with a partial reduction of Pt(IV) to Pt(II) and the oxidation of the polypyrrol polymeric chain. Table 2 shows an increase of the -NH- contribution respective to =N- in PPy-2%Pt, when compared with PPy. The XPS spectra corresponding to the Pt 4f level of polypyrrole impregnated with H_2PtCl_6 can be deconvoluted into two bands (Fig. 4, Supporting information Table 5), at 74.0 eV ($Pt4f_{7/2}$) and 77.4 eV ($Pt4f_{5/2}$), which correspond to Pt(IV), and two other at 72.9 eV ($Pt4f_{7/2}$) and 76.1 eV ($Pt4f_{5/2}$), which correspond to Pt(II), which is the predominant species. The absence of metallic platinum, which should appear at lower binding energies, is confirmed. XPS spectra of polypyrrole co-impregnated with H_2PtCl_6 and $SnCl_2$ show the presence of Pt ions, as Pt(IV) and Pt(II), and tin ions (it is not possible to discern between both oxidation stated by XPS analysis) (Fig. 4, Supporting information Table 5). There is also a shift of the N 1s band to higher binding energies, and N^+ at 401.9 eV is detected (Fig. 3). When the Sn content increases, Pt(IV) becomes dominant compared to the Pt(II) contribution, and the N^+/-NH- ratio is also affected, *i.e.* 1.41 for Pt:Sn (3:1) and 0.16 for Pt:Sn (1:1) (Fig. 3, Supporting information Table 4). This suggests that the reduction of Pt(IV) to Pt(II) becomes hindered as the amount of tin increases, and, consequently, the polymeric chain also results in a lower oxidation degree (evaluated from the N^+/-NH- ratio). Therefore, it may be concluded that the presence of ionic tin species modifies the extent of electron transfer from the nitrogen atoms in the polymeric chain to platinum ions anchored as platinum chloro-complex.

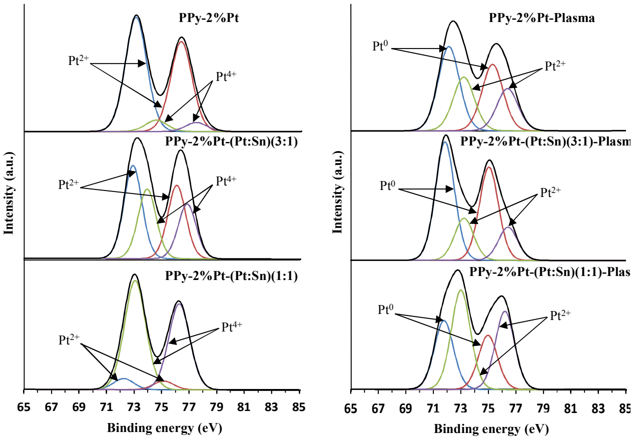

Fig. 4. Curve fit of Pt 4f level in XPS spectra of different samples.

Table 2. Atomic ratios (XPS) of the different surface species.

Sample[a]	C/O	-NH/=N-	N^+/-NH-	Pt^0/Pt^{n+}
PPy-2%Pt-(Pt:Sn)(1:1)	5.31	-	0.16	-
PPy-2%Pt-(Pt:Sn)(1:1)-P	3.41	-	0.34	0.70
PPy-2%Pt-(Pt:Sn)(1:1)-P-R	3.35	-	2.21	0.49
PPy-2%Pt-(Pt:Sn)(3:1)	16.14	-	1.41	-
PPy-2%Pt-(Pt:Sn)(3:1)-P	4.46	-	0.18	2.81
PPy-2%Pt-(Pt:Sn)(3:1)-P-R	4.48	-	3.25	1.50
PPy-2%Pt	14.81	2.68	-	-
PPy-2%Pt-P	4.73	3.57	-	1.57
PPy-2%Pt-P-R	6.33	2.44	-	-
PPy	11.96	1.83	-	-
PPy-R	7.56	3.87	-	-
PPy-Plasma	5.07	-	0.10	-
PPy-Plasma-R	5.37	2.92	-	-

[a] P = plasma; R = recovered catalysts after 300 min of reaction of nitrate reduction with hydrogen.

For most platinum-catalyzed reactions, the presence of platinum in its zero-state is required. Thus, the reducing capability of the Ar plasma treatment was analyzed by XPS. Previous studies[23] have shown the capability of Ar plasma to partially reduce platinum ions in monometallic polypyrrole-supported catalysts. Pt 4f curve fit (Fig. 4, Supporting information Table 5) shows that argon plasma produces partial reduction of platinum ions into metallic platinum and Pt(IV) is not further present. However, no metallic tin is detected, although it has to be taken into account that it could be produced upon the plasma treatment but re-oxidized during the subsequent air exposure. Besides, Ar plasma treatment activates polypyrrole surface in such a way that ulterior contact with air favors the creation of oxygenated moieties. Accordingly, the C/O ratio decreased after argon plasma treatment (Table 2). Ar plasma treatment also produces ablation of the polypyrrole surface and, as a result of this, platinum and tin located within the polymer network were exposed to the outermost polypyrrole surface and were detected by XPS, with the consequent increase of surface Pt and Sn percentages (Supporting information Table 1). Consequently, an improvement of efficiency of these catalysts after plasma treatment is expected.

TEM images of platinum and platinum-tin impregnated-polypyrrole (Fig. 5) show a good dispersion of metal nanoparticles. Plasma treatment produced only a slight aggregation of nanoparticles, although in all cases the particle sizes were smaller than 5 nm. As a consequence of high dispersion, no metallic platinum is detected by X-ray diffraction (Fig. 1), although Pt(0) was detected by XPS on plasma treated samples.

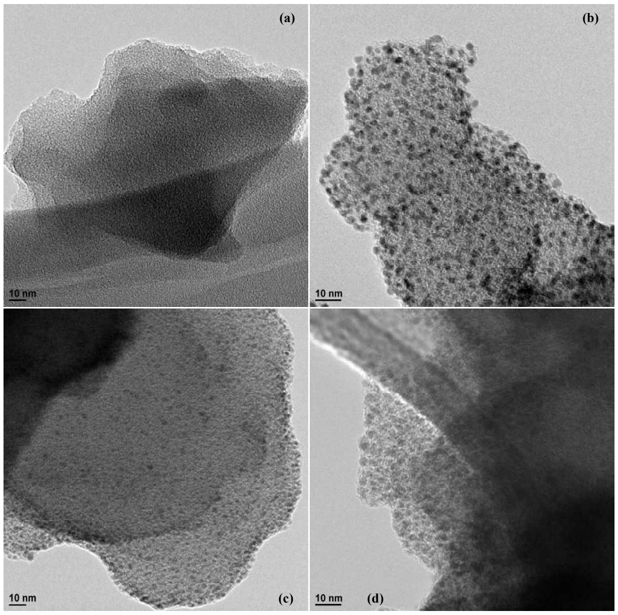

Fig. 5. TEM images of (a) PPy-Plasma, (b) PPy-2%Pt-Plasma, (c) PPy-2%Pt-(Pt:Sn)(3:1)–Plasma and (d) PPy-2%Pt-(Pt:Sn)(1:1)-Plasma.

Catalytic behaviour

A control reaction was carried out flowing H_2 (reducing agent) and CO_2 (buffer) through the aqueous nitrate solution. Aliquots were periodically extracted and analyzed by ion chromatography. After 300 min, nitrate concentration remained unmodified and neither nitrite nor ammonium was detected. This indicates that the reaction did not run in the absence of a catalyst. In order to elucidate the role of the polymeric support in the removal of nitrates from water, the polymer was put into contact with the aqueous nitrate solution in the presence of CO_2 (buffer) flow. No metal catalyst or reducing agent was added. A considerable decrease of nitrate concentration was observed, but no nitrite was detected and only a very small ammonium concentration was detected after 300 min (Fig. 6).

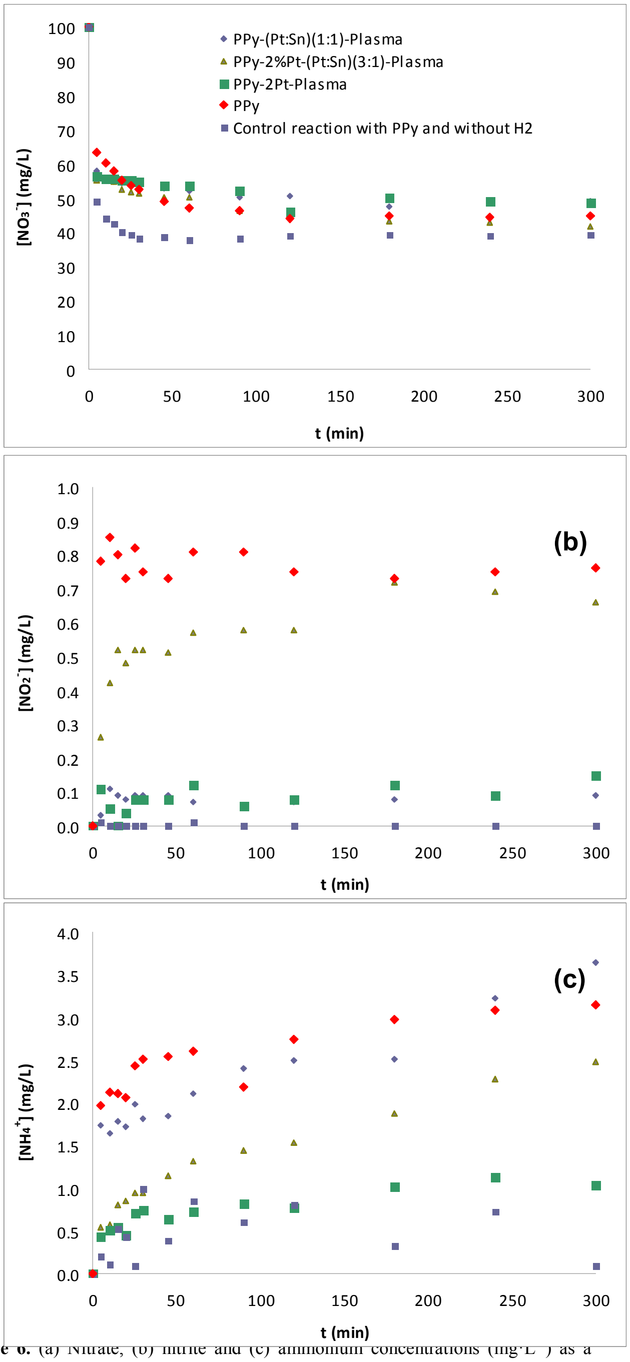

Figure 6. (a) Nitrate, (b) nitrite and (c) ammonium concentrations (mg·L^{-1}) as a function of time (min) during aqueous nitrate reduction with hydrogen in the presence of three different catalysts.

Table 3. Nitrate, nitrite and ammonium concentrations, nitrate conversion and selectivities to nitrite and ammonium after 300 min of nitrate reduction with hydrogen.

Sample[a]	(mg·L^{-1})			(%)		
	[NO_3^-]	[NO_2^-]	[NH_4^+]	$X_{NO_3^-}$	$S_{NO_2^-}$	$S_{NH_4^+}$
PPy-2%Pt-(Pt:Sn)(1:1)-P	48.9	0.1	3.7	51	0.2	24.3
PPy-2%Pt-(Pt:Sn)(3:1)-P	41.8	0.7	2.5	58	1.5	14.6
PPy-2%Pt-P	48.8	0.2	1.0	51	0.4	7.0
PPy	44.7	0.8	3.1	55	1.9	19.4
PPy control no H_2	39.7	0	0.1	61	0	0.6

[a] P = plasma

The mechanism of nitrate abatement on these systems could at first be explained by ion exchange between Cl^- (as doped polypyrrole counter-ion) and NO_3^-. However, if a simple ion exchange occurred, nitrate would be present at the polymeric support after the reaction. But recovered PPy after 300 min in contact with nitrate solution did not show NO_3^- contribution to N1s (XPS) at 406 eV. Considering the redox potentials for the implied species (PPy^+/PPy, E° = 0.150 V; NO_3^-/NH_4^+, E° = 0.875 V; NO_3^-/N_2, E° = 1.246 V), (Scheme 1) reduction of nitrate is expected to be produced by electrons coming from the polypyrrole chain. Thus, nitrate would be reduced to nitrogen (assuming that the amount of other nitrogen species eventually produced is negligible)[4] and only a small part would be reduced to ammonium. Consequently, PPy which is initially in its reduced state as assesed by XPS (4.65 at% of =N- at 399.7 and 8.51 at% of -NH- at 400.3 eV in Supporting information Table 4) shows oxidation of its nitrogen species when is recovered after being in contact with a nitrate solution in a CO_2 flow for 300 min (9.31 at% of –NH- at 400.05 eV and 0.52 at% of N^+ at 401.27 eV).

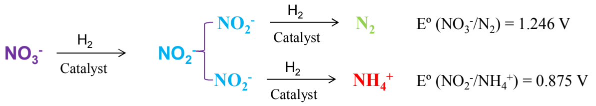

Scheme 1. Reaction pathways and redox potentials for aqueous nitrate reduction by hydrogen.

A similar experiment was performed, but in the presence of hydrogen as reductor. Thus PPy was put into contact with the aqueous nitrate solution in the presence of CO_2 and H_2. Nitrate abatement from solution in the presence of hydrogen acting as reductor is not as effective as nitrate removal by the polymer in the absence of hydrogen. Nevertheless, measured nitrate concentration is below 50 mg ·L^{-1} (Fig. 6). Nitrogen species in recovered PPy are in its reduced state (2.43 at% of =N- and 9.41 at% of -NH-) as in the pristine PPy (4.65 at% of =N- and 8.51 at% of -NH-), this suggesting that the main reductor in this case has been hydrogen. However, considerable amounts of nitrite and ammonium are detected. Consequently, in order to minimize NO_2^- and NH_4^+ production, it is necessary to catalyze the selective reduction of NO_3^- to N_2. Therefore, the activity and selectivity of the polypyrrole-supported platinum and platinum-tin catalysts was evaluated.

Previous studies[6,30] stated that Pd or Pt monometallic catalysts catalyze reduction of nitrite (NO_2^-), but a promoter is necessary for the reduction of nitrate (NO_3^-) when carbon materials are used as support. However, in this study, nitrate concentration in water below the maximum acceptable level of 50 mg·L^{-1} (91/676/CEE European legislation) is achieved with all studied mono- and bimetallic catalysts (Fig. 6, Table 3).

The most important decrease of nitrate concentration in water was achieved with PPy-2%Pt-(Pt:Sn)(3:1)-Plasma bimetallic catalyst, which was the one with the highest metallic platinum content, as estimated by XPS analysis (Pt^o/Pt^{2+}= 2.81; Table 2). However, with this catalyst, nitrate reduction progresses through the non-desired nitrite intermediate (maximum acceptable nitrite level in water is 0.5 mg·L^{-1}). On the other hand, ammonium concentration is higher with the PPy-2%-(Pt:Sn)(1:1)-Plasma catalyst (Pt^o/Pt^{2+} = 0.70; Table 2). However, considering not only the efficiency in nitrate reduction, but also the minimized concentrations of the undesired intermediate (nitrite) and by-product (ammonium), the monometallic Pt-Plasma catalyst seems to be the most promising one. At this point, is interesting to note that ICP-MS results (Table 4) show that neither platinum nor tin leaching was produced, as lixiviated metal (platinum or tin) is less than 0.1%.

Recovered catalysts after 300 min reaction have been analyzed by XPS. A decrease of Cl and Pt contents was observed in all cases (Supporting information Table 1). The XPS spectra for the N 1s level of the recovered bimetallic catalysts (Table 2) show that there is an increase of the N^+/-NH- ratio in polypyrrole, which supports the hypothesis that the polymeric support participates in the reduction reaction. As suggested before, a possible mechanism would be an ion exchange between the Cl^- counter-ion present in polypyrrole doped with $FeCl_3$ by NO_3^- from solution. This is supported by the fact that the Cl content estimated from XPS analysis is lower in recovered catalysts. Then, polypyrrole in its reduced state might donate electrons to nitrate, which reduces to nitrogen and/or ammonium. The electron donation degree is influenced by the presence of ionic tin species. XPS spectra of the Sn 3d level show that no metallic tin is detected, but it is not possible to discern between Sn(II) and Sn(IV) species. Besides, there is a decrease of the metallic platinum/ionic platinum ratio in the recovered bimetallic catalysts, and no metallic Pt is detected on the surface of the recovered monometallic catalyst (Table 2). These findings suggest that during the nitrate reduction reaction, a given amount of metallic platinum supported on polypyrrole is oxidized to ionic platinum (as polypyrrole chain is reduced). Polypyrrole chain can act as a source and drain of electrons, donating electrons to nitrate, which become reduced, and accepting electrons from metallic platinum, which oxidizes to different extent depending on ionic tin being present or not. Ionic tin affects in someway the electron transfer from and towards the polymeric chain; this explains that the XPS N 1s band is shifted to higher binding energies in the bimetallic catalysts, compared to monometallic one. Thus, the balance between two processes, Cl^-/NO_3^- exchange and electron transfer between hydrogen, polypyrrole, platinum and nitrate, may be modified depending on the presence of the platinum catalyst and the tin promoter.

Table 4. Concentration of lixiviated (l) and theoretical (T) metals detected by ICP-MS in solution after 300 min of reaction of nitrate reduction with hydrogen.

Sample[a]	(ppb)		% Pt_l	(ppb)		% Sn_l
	$[Pt]_l$	$[Pt]_T$		$[Sn]_l$	$[Sn]_T$	
PPy-2%Pt-(Pt:Sn)(3:1)-P	3.630	$1.031 \cdot 10^4$	0.035	0.816	$2.138 \cdot 10^3$	0.038
PPy-2%Pt-P	2.061	$1.129 \cdot 10^4$	0.018	-	-	-

[a] P = plasma

Conclusions

Pt and Pt:Sn catalysts supported on polypyrrole have been prepared using environmentally-friendly argon plasma treatment, which produced a partial reduction of platinum ions, anchored as a platinum chloro-complex to the polypyrrole chain, into metallic platinum, but it did not reduce ionic tin to its metallic state. Furthermore, this treatment activated the polypyrrole surface and subsequent exposure to air produced C=O moieties. An indirect process involving the water molecules within the polymer network led to the creation of C=O and RO-C=O moieties under plasma treatment.

The polymeric support suffered ion exchange of Cl^- counter ions by NO_3^- from reaction solution, and also participated in the redox process of nitrate reduction. Supported metals catalyze this process, so kinetics of the reduction reaction of nitrates anchored to polypyrrol is increased.

All the prepared catalysts were effective in the reduction of aqueous nitrate with H_2 at room temperature, and nitrate concentrations in water below the maximum acceptable level of 50 $mg \cdot L^{-1}$ were achieved with all catalysts. However, considering not only the efficiency in nitrate reduction, but also minimized concentrations of the undesired intermediate (nitrite) and by-product (ammonium), the monometallic Pt catalyst seems to be the most promising one.

A balance between two processes, Cl^-/NO_3^- exchange and electron transfer between polypyrrole, platinum and nitrate, can be modified depending on the presence of the platinum catalyst and the tin promoter.

Acknowledgements

Financial support from Generalitat Valenciana, Spain (PROMETEO/2009/002 – FEDER and PROMETEOII/2014/004) is gratefully acknowledged. Support by PEst-C/EQB/LA0020/2013, financed by FEDER through COMPETE - Programa Operacional Factores de Competitividade, and by FCT - Fundação para a Ciência e a Tecnologia; NORTE-07-0162-FEDER-000050, financed by QREN, ON2 and FEDER is acknowledged by LCM group. O.S.G.P. Soares acknowledges the grant received from FCT (SFRH/BPD/ 97689/2013).

References

1 T.E. Arbuckle, G.J. Sherman, P.N. Corey, D. Walters, B. Lo, *Arch. Environ. Health,* 1988, **43(2)**, 162.
2 ECETOC (European Chemical Industry Ecology and Toxicology Center). *Technical Report No. 27, Nitrate and drinking water*. Brussels, Belgium, 1988.
3 U.S. EPA. *Criteria Document for Nitrate/Nitrite.* Office of Drinking Water, Washington, DC, 1990.
4 R. Zhang, D. Shuai, K.A. Guy, J.R. Shapley, T.J. Strathmann, C.J. Werth, *ChemCatChem* 2013, **5**, 313.
5 I. Dodouche, F. Epron, *Applied Catalysis B: Environmental* 2007, **76**, 291.
6 I. Dodouche, D.P. Barbosa, M.C. Rangel, F. Epron, *Applied Catalysis B: Environmental* 2009, **93**, 50.
7 O.S.G.P. Soares, J.J.M. Órfão, M.F.R. Pereira, *Desalination*, 2011, **279***,* 367.
8 O.S.G.P. Soares, J.J.M. Órfão, M.F.R. Pereira, *Industrial & Engineering Chemistry Research* 2010, **49**, 7183.
9 J. Sá, J.A. Anderson, *Applied Catalysis B: Environmental*, 2008, **77**, 409.
10 A. Garron, K. Lazar, F. Epron, *Applied Catalysis B: Environmental*, 2005, **59**, 57.
11 M.P. Maia, M.A. Rodrigues, F.B. Passos, *Catalysis Today,* 2007, **123**, 171.
12 M. D'Arino, F. Pinna, G. Strukul, *Applied Catalysis B: Environmental*, 2004, **53**, 161.
13 Z.Y. Xu, L.Q. Chen, Y. Shao, D.Q. Yin, S.R. Zheng, *Industrial & Engineering Chemistry Research*, 2009, **48**, 8356.
14 F. Epron, F. Gauthard, C. Pineda, J. Barbier, *Journal of Catalysis*, 2001, **198**, 309.
15 J. Sa, C.A. Agüera, S. Gross, J.A. Anderson, *Applied Catalysis B: Environmental*, 2009, **85**, 192,.
16 F. Epron, F. Gauthard, J. Barbier, *Journal of Catalysis*, 2002, **206**, 363,.
17 K. Nakamura, Y. Yoshda, I. Mikami, T. Okuhara, *Applied Catalysis B: Environmental*, 2006, **65**, 31.
18 A.E. Palomares, J.G. Prato, F. Rey, A. Corma, *Journal of Catalysis*, 2004, **221**, 62,
19 O.S.G.P. Soares, J.J.M. Órfão, M.F.R. Pereira, *Applied Catalysis B: Environmental*, 2011, **102**, 424.
20 U. Prusse, K.D. Vorlop, *Journal of Molecular Catalysis A: Chemical* 2001, **173**, 313.
21 K. Wada, T. Hirata, S. Hosokawa, S. Iwamoto, M. Inoue, *Catalysis Today*, 2012, **185**, 81.
22 K. Nakamura, Y. Yoshida, I. Mikami, T. Okuhara, *Applied Catalysis B: Environmental*, 2006, **65**, 31.
23 R. Buitrago-Sierra, M.J. García-Fernández, M.M. Pastor-Blas, A. Sepúlveda-Escribano, *Green Chemistry*, 2013, **15**, 1981.
24 S.-S. Kim, H. Lee, H.-K. Song, *Catalysis Today* 2004, **89**, 193.
25 K. Cheah, M. Forsyth, V.T. Truong, *Synthetic Metals* 1999, **101**, 19.
26 P. Mavinakuli, S. Wei, Q. Wang, A.B. Karki, S. Dhage, Z. Wang, D.P. Young, Z. Guo, *Journal of Physical Chemistry C*, 2010, **114***,* 3874.
27 T.A. Skotheim, J.R. Reynolds, *Handbook of conducting polymers. Conjugated polymers. Theory, synthesis, properties, and characterization*, *Chap. 8* (3rd Ed.), CRC Press, 2007.
28 N. Dubey, M. Leclerc, *Journal of Polymer Science Part B: Polymer Physics*, 2011, **49**, 467.
29 B. Sari, M. Talu, *Synthetic Metals*, 1998, **94**, 221.
30 O.S.G.P. Soares, E.O. Jardim, A. Reyes-Carmona, J. Ruiz-Martínez, J. Silvestre-Albero, E. Rodríguez-Castellón, J.J.M. Órfão, A. Sepúlveda-Escribano, M.F.R. Pereira, *Journal of Colloid and Interface Science*, 2012, **369**, 294.

Notes

[(a)] *Laboratorio de Materiales Avanzados, Departamento de Química Inorgánica-Instituto Universitario de Materiales de Alicante, Universidad de Alicante, Apartado 99, E-03080 Alicante. Spain.*
Fax: +34 965903454; Tel:+34 965903974; E-mail: asepul@ua.es
[(b)] *Laboratório de Catálise e Materiais (LCM. Laboratório Associado LSRE/LCM.Departamento de Engenharia Química.Faculta de de Engenharia.Universidade do Porto.Rua Dr. Roberto Frias. 4200-465 Porto, Portugal..E-mail: fpereira@fe.up.pt*

† Electronic Supplementary Information (ESI) available: [details of any supplementary information available should be included here]. See DOI: 10.1039/b000000x/